



Cell-Type Specific Neuromodulation of Excitatory and Inhibitory Neurons via Muscarinic Acetylcholine Receptors in Layer 4 of Rat Barrel Cortex

Guanxiao Qi^{1*} and Dirk Feldmeyer^{1,2,3*}

¹ Institute of Neuroscience and Medicine, INM-10, Research Centre Jülich, Jülich, Germany, ² Department of Psychiatry, Psychotherapy and Psychosomatics, RWTH Aachen University, Aachen, Germany, ³ Jülich-Aachen Research Alliance-Brain, Translational Brain Medicine, Aachen, Germany

OPEN ACCESS

Edited by:

Yoshiyuki Kubota,
National Institute for Physiological
Sciences (NIPS), Japan

Reviewed by:

Michael M. Kohl,
University of Glasgow,
United Kingdom
Rheinallt Parri,
Aston University, United Kingdom

*Correspondence:

Guanxiao Qi
g.qi@fz-juelich.de
Dirk Feldmeyer
d.feldmeyer@fz-juelich.de

Received: 24 December 2021

Accepted: 27 January 2022

Published: 18 February 2022

Citation:

Qi G and Feldmeyer D (2022)
Cell-Type Specific Neuromodulation
of Excitatory and Inhibitory Neurons
via Muscarinic Acetylcholine
Receptors in Layer 4 of Rat Barrel
Cortex.
Front. Neural Circuits 16:843025.
doi: 10.3389/fncir.2022.843025

The neuromodulator acetylcholine (ACh) plays an important role in arousal, attention, vigilance, learning and memory. ACh is released during different behavioural states and affects the brain microcircuit by regulating neuronal and synaptic properties. Here, we investigated how a low concentration of ACh (30 μ M) affects the intrinsic properties of electrophysiologically and morphologically identified excitatory and inhibitory neurons in layer 4 (L4) of rat barrel cortex. ACh altered the membrane potential of L4 neurons in a heterogeneous manner. Nearly all L4 regular spiking (RS) excitatory neurons responded to bath-application of ACh with a M4 muscarinic ACh receptor-mediated hyperpolarisation. In contrast, in the majority of L4 fast spiking (FS) and non-fast spiking (nFS) interneurons 30 μ M ACh induced a depolarisation while the remainder showed a hyperpolarisation or no response. The ACh-induced depolarisation of L4 FS interneurons was much weaker than that in L4 nFS interneurons. There was no clear difference in the response to ACh for three morphological subtypes of L4 FS interneurons. However, in four morpho-electrophysiological subtypes of L4 nFS interneurons, VIP+-like interneurons showed the strongest ACh-induced depolarisation; occasionally, even action potential firing was elicited. The ACh-induced depolarisation in L4 FS interneurons was exclusively mediated by M1 muscarinic ACh receptors; in L4 nFS interneurons it was mainly mediated by M1 and/or M3/5 muscarinic ACh receptors. In a subset of L4 nFS interneurons, a co-operative activation of muscarinic and nicotinic ACh receptors was also observed. The present study demonstrates that low-concentrations of ACh affect different L4 neuron types in a cell-type specific way. These effects result from a specific expression of different muscarinic and/or nicotinic ACh receptors on the somatodendritic compartments of L4 neurons. This suggests that even at low concentrations ACh may tune the excitability of L4 excitatory and inhibitory neurons and their synaptic microcircuits differentially depending on the behavioural state during which ACh is released.

Keywords: acetylcholine, layer 4, barrel cortex, muscarinic acetylcholine receptor, nicotinic acetylcholine receptor

INTRODUCTION

Normal brain function relies on the participation of diverse neuromodulators such as the acetylcholine (ACh), noradrenaline, dopamine, and serotonin. These neuromodulators are mainly released from different subcortical brain regions during different cognitive and behavioural states and affect neuronal microcircuits differently yet in a collaborative way. ACh plays a critical role in many cognitive functions including arousal, attention, vigilance, learning, and memory (Hasselmo, 2006; Picciotto et al., 2012; Colangelo et al., 2019). While ACh is mainly released from axonal boutons of neurons located in the nucleus basalis of Meynert in the basal forebrain (Mesulam et al., 1983; Zaborszky et al., 2015), it may also be co-released from neocortical choline acetyltransferase (ChAT)-expressing/vasoactive intestinal peptide (VIP)-positive interneurons together with the inhibitory transmitter GABA and/or VIP (Obermayer et al., 2019; Granger et al., 2020). ACh effects are mediated by two different types of receptors, the G-protein-coupled muscarinic ACh receptors (mAChRs) and the ionotropic nicotinic ACh receptors (nAChRs). In the neocortex, both receptor types show layer-specific distributions and effects (Obermayer et al., 2017; Radnikow and Feldmeyer, 2018). In general, ACh increases the excitability of pyramidal cells located in different cortical layers by activating both nAChRs and mAChRs (Gulledge et al., 2007; Zolles et al., 2009; Bailey et al., 2010; Tian et al., 2014; Hay et al., 2016; Yang et al., 2020; Patel et al., 2021). In a minor fraction of deep L2/3 and a subset of L5/6 pyramidal cells, ACh induces an initial small and transient hyperpolarisation followed by a sustained depolarisation mediated by muscarinic M1/3 mAChRs (Gulledge and Stuart, 2005; Gulledge et al., 2007; Eggermann and Feldmeyer, 2009; Patel et al., 2021). In contrast, excitatory neurons located in layer 4 are persistently hyperpolarised by ACh activating M4 mAChRs (Eggermann and Feldmeyer, 2009; Dasgupta et al., 2018). A similar ACh effect was also found in L6A corticocortical neurons (Yang et al., 2020).

Cholinergic effects on GABAergic inhibitory interneurons are heterogenous and dependent on interneuron subtypes (Bacci et al., 2005; Muñoz and Rudy, 2014). Cortical interneurons can be broadly divided into two large groups according to their firing patterns, i.e., fast spiking (FS) and non-FS (nFS) interneurons. ACh induces a depolarisation in the majority of nFS interneurons [e.g., somatostatin-expressing (SST+) adapting firing, VIP+ irregular spiking interneurons] *via* the activation of nAChRs and/or mAChRs but induces a hyperpolarisation in others such as cholecystokinin-expressing (CCK+) regular spiking interneurons (Kawaguchi, 1997; Gulledge et al., 2007). Whether FS interneurons show ACh effects is still a matter of debate (Kawaguchi, 1997; Xiang et al., 1998; Gulledge et al., 2007; Kruglikov and Rudy, 2008; Chen et al., 2015).

The ACh response of a neuron depends on the concentration and the speed and spatial profile of application. In the majority of studies, a high concentration of ACh (~1 mM) was applied locally through a puff pipette; this approach reveals predominantly the nicotinic ACh response but largely obscures any muscarinic ACh effects. Furthermore, a puff-application mimics (to some extent) phasic ACh release on a short time

scale (within a few ms) but does not simulate tonic, non-synaptic ACh release into the extracellular space, the so-called “volume transmission” (Fuxe and Borroto-Escuela, 2016).

In sensory cortices, L4 neurons receive direct thalamocortical input and distribute intracortical excitation and inhibition to other cortical layers. While the neuronal composition and synaptic connectivity of layer 4 have been studied extensively (Feldmeyer et al., 1999; Gibson et al., 1999; Lubke et al., 2000; Beierlein et al., 2003; Xu et al., 2013; Koelbl et al., 2015; Emmenegger et al., 2018; Scala et al., 2019) a comprehensive study on their modulation by ACh or other neuromodulators is still lacking. Here, we investigated how low concentrations of ACh affect the intrinsic properties of different L4 neuron types and subtypes in acute brain slices using patch-clamp recordings and bath-application of cholinergic agonists and antagonists. To reveal the cell-type specific effects of ACh, L4 neurons were classified into three electrophysiological types and ten electromorphological subtypes as identified previously (Feldmeyer et al., 1999; Staiger et al., 2004; Koelbl et al., 2015; Emmenegger et al., 2018). We found that neuromodulation by mAChRs is a common property of all L4 neurons but is highly cell type-specific. Furthermore, in some L4 nFS interneuron types low concentrations of ACh evoked a strong superthreshold depolarisation mediated by coincident activation of both mAChRs and nAChRs suggesting a cooperative interaction of the two receptor types in cholinergic modulation of neuronal excitability and synaptic transmission.

MATERIALS AND METHODS

All experimental procedures involving animals were performed in accordance with the guidelines of the Federation of European Laboratory Animal Science Association (FELASA), the EU Directive 2010/63/EU, and the German animal welfare law.

Slice Preparation

In this study, Wistar rats (Charles River, either sex) aged 18–33 postnatal days (P18–P33) were maintained on a 12/12-h light/dark cycle with lights on from 7 a.m. to 7 p.m. Rats were anaesthetized with isoflurane at a concentration <0.1% and decapitated between 10:30 a.m. and 11:30 a.m. The brain was quickly removed and placed in an ice-cold modified artificial cerebrospinal fluid (ACSF) containing a high Mg^{2+} and a low Ca^{2+} concentration (4 mM $MgCl_2$ and 1 mM $CaCl_2$), other components are same to that in the perfusion ACSF as described below, to reduce potentially excitotoxic synaptic transmission during slicing. In order to maintain adequate oxygenation and a physiological pH level, the solution was constantly bubbled with carbogen gas (95% O_2 and 5% CO_2). Thalamocortical slices (Feldmeyer et al., 1999; Qi et al., 2017) were cut at 350 μm thickness using a Leica VT1000S vibrating blade microtome and then transferred to an incubation chamber containing preparation solution for a recovery period of at least 30 min at room temperature before being transferred to the recording chamber. After cutting, slices from animals older than P21 were transferred to a holding chamber placed in a water bath at 35°C

for 30 min and then, the water bath was allowed to gradually cool down to the room temperature.

Solution

During recordings, slices were continuously superfused (perfusion speed ~ 5 ml/min) with ACSF containing (in mM): 125 NaCl, 2.5 KCl, 1.25 NaH_2PO_4 , 1 MgCl_2 , 2 CaCl_2 , 25 NaHCO_3 , 25 D-glucose, 3 mho-inositol, 2 sodium pyruvate, and 0.4 ascorbic acid, bubbled with carbogen gas (95% O_2 and 5% CO_2) and maintained at 30–33°C. Patch pipettes (5–8 M Ω) were pulled from thick-wall borosilicate glass capillaries and filled with an internal solution containing (in mM): 135 K-gluconate, 4 KCl, 10 HEPES, 10 phosphocreatine, 4 Mg-ATP, and 0.3 GTP (pH 7.4 with KOH, 290–300 mOsm). Biocytin at a concentration of 5 mg/ml was added to the internal solution in order to stain patched neurons after recordings.

Electrophysiological Recording and Analysis

Slices and neurons were visualised using an upright microscope equipped with an infrared differential interference contrast (IR-DIC) optics. The barrels can be identified in layer 4 as dark stripes with light “hollows” at low magnification (4 \times objective) and were visible in 6–8 consecutive slices. Neurons located inside the barrels were randomly selected for recordings. When being visualised at high magnification (40 \times magnification), putative excitatory neurons have ovoid-shape somata without obvious apical dendrites and putative interneurons have enlarged oval somata. They could also be differentiated by their action potential (AP) firing patterns during recording and by their morphological appearances thereafter. Whole-cell patch clamp recordings were made using an EPC10 amplifier (HEKA, Lambrecht, Germany). Signals were sampled at 10 kHz, filtered at 2.9 kHz using Patchmaster software (HEKA), and later analysed off-line using Igor Pro software (WaveMetrics, United States).

Custom-written macros in Igor Pro 6 (WaveMetrics, Lake Oswego, OR, United States) were used to analyse the recorded electrophysiological signals. Passive and active AP firing properties were assessed by eliciting a series of 1 s current pulses under current clamp configuration. The series resistance and capacitance were carefully adjusted after breaking through the membrane into whole-cell mode and continuously compensated by 80% during recordings. Membrane potentials were not corrected for a junction potential. Neurons with a series resistance exceeding 40 M Ω or with a depolarized resting membrane potential (> -55 mV) after rupturing the cell membrane were excluded from analysis. The resting membrane potential (V_{rest}) was recorded immediately after establishing the whole-cell recording configuration. Other passive membrane properties such as the input resistance R_{in} , membrane time constant τ_m , voltage sag were measured from membrane potential (V_m) traces induced by a series of hyper- and depolarizing subthreshold current pulses. Single AP properties such as the AP threshold, amplitude, half-width, afterhyperpolarisation (AHP) amplitude were measured for the first spike elicited by a rheobase current step. Repetitive

firing properties such as the maximum firing frequency, slope of frequency-current curve were measured. The description of most electrophysiological parameters for data analysis has been described previously (Emmenegger et al., 2018).

Drug Application and Analysis

Acetylcholine (30 μM) was applied through the perfusion system. Atropine (ATRO, 200 nM), mecamylamine (MEC, 10 μM), tropicamide (TRO, 1 μM), pirenzepine (PIR, 0.5 μM), dihydro- β -erythroidine (DH β E, 10 μM), TTX (0.5 μM) and the cocktail of synaptic blockers including CNQX (10 μM), D-AP5 (50 μM), gabazine (10 μM) were all bath-applied; drugs were purchased from Sigma-Aldrich or Tocris. During recordings, a 3 min stable baseline with a V_m fluctuation < 1 mV was recorded before applying the drug *via* the perfusion system. The change in V_m was calculated as the difference between the maximum V_m deflection (positive or negative) after drug application and the baseline. To avoid a misclassification of the V_m change because of background V_m fluctuation, we set a threshold of ± 0.5 mV so that a V_m change ≤ 0.5 mV during drug application is considered to be no response.

Immunohistochemical Staining

Slices were fixed after electrophysiological recordings with 4% paraformaldehyde in 100 mM phosphate buffered saline (PBS) for at least 24 h at 4°C. To recover the morphology of biocytin-filled neurons, slices were rinsed several times in 100 mM PBS and then treated with 1% H_2O_2 in PBS for about 20 min in order to reduce any endogenous peroxidase activity. Slices were rinsed repeatedly with PBS and then incubated in 1% avidin-biotinylated horseradish peroxidase (Vector ABC staining kit, Vector Lab. Inc., Burlingame, CA, United States) containing 0.1% Triton X-100 for 1 h at room temperature. The reaction was catalysed using 0.5 mg/ml 3,3-diaminobenzidine (DAB; Sigma-Aldrich, St. Louis, MO, United States) as a chromogen. Slices were then rinsed with 100 mM PBS, followed by slow dehydration with ethanol in increasing concentrations and finally in xylene for 2–4 h. After that, slices were embedded using Eukitt medium (Otto Kindler GmbH, Freiburg, Germany).

Morphological Reconstruction and Analysis

Computer-assisted morphological 3D reconstructions of neurons were made using the NEUROLUCIDA[®] software (MicroBrightField, Williston, VT, United States) and Olympus BV61 microscopy at 1000 \times magnification (100 \times objective, 10 \times eyepiece). Neurons were selected for reconstruction based on the quality of biocytin labelling when background staining was minimal. The cell body, dendritic and axonal branches were reconstructed manually under constant visual inspection to detect thin and small collaterals. Cytoarchitectonic landmarks such as barrels in the primary somatosensory cortex and layer borders, pial surface and white matter were delineated during reconstructions at a low magnification (4 \times objective). The position of soma and layers were confirmed by superimposing the DIC images taken during the recording. Tissue shrinkage was

corrected using correction factors of 1.1 in the x–y direction and 2.1 in the z direction (Marx et al., 2012).

Statistical Analysis

For all data, the mean \pm s.d. is given. Statistical comparisons among multiple groups were done using a Kruskal–Wallis test followed by a Dunn–Holland–Wolfe non-parametric multiple comparison test. Wilcoxon Mann–Whitney *U* test was performed to assess significant differences between individual groups. To assess the differences between two paired groups under different pharmacological conditions, Wilcoxon signed-rank test was performed. Correlation analysis was performed by calculating Pearson's linear correlation coefficients. Statistical significance was set at $p < 0.05$, *n* indicates the number of neurons analysed. To prepare box plots for dataset with $n > 10$, the web application PlotsOfData was used¹ (Postma and Goedhart, 2019). In box plots, the interquartile range (IQR) is shown as a box, the range of values that are within 1.5*IQR are shown as whiskers and the median is represented by a horizontal line in the box.

RESULTS

We performed single-cell patch-clamp recordings in combination with biocytin fillings in acute brain slices to characterise the modulatory effect of ACh on the intrinsic properties of L4 neurons in the primary somatosensory (barrel) cortex of rats. In total, we have tested the effects of a low concentration of ACh (30 μ M) on 108 L4 excitatory and inhibitory neurons. The ACh responses of L4 neurons was highly diverse depending on their electrophysiological and morphological identities.

Electro-Morphological Classification of Layer 4 Neurons

Based on their electrophysiological characteristics, L4 neurons can be broadly classified as regular spiking (RS) excitatory neurons, FS and nFS inhibitory interneurons (Figure 1A). Three L4 neuron types can be easily differentiated by only three electrophysiological parameters, i.e., the maximum firing frequency, AP half-width and the AHP amplitude (Figures 1B,C). L4 RS neurons show a regular spiking firing pattern with a prominent spike frequency adaptation during a 1 s depolarising pulse (Figures 1B,C). In contrast, L4 FS interneurons show a high-frequency firing pattern without obvious spike frequency adaptation. L4 interneurons of the nFS type show heterogeneous firing patterns including adaptive spiking, irregular spiking, late spiking, etc.

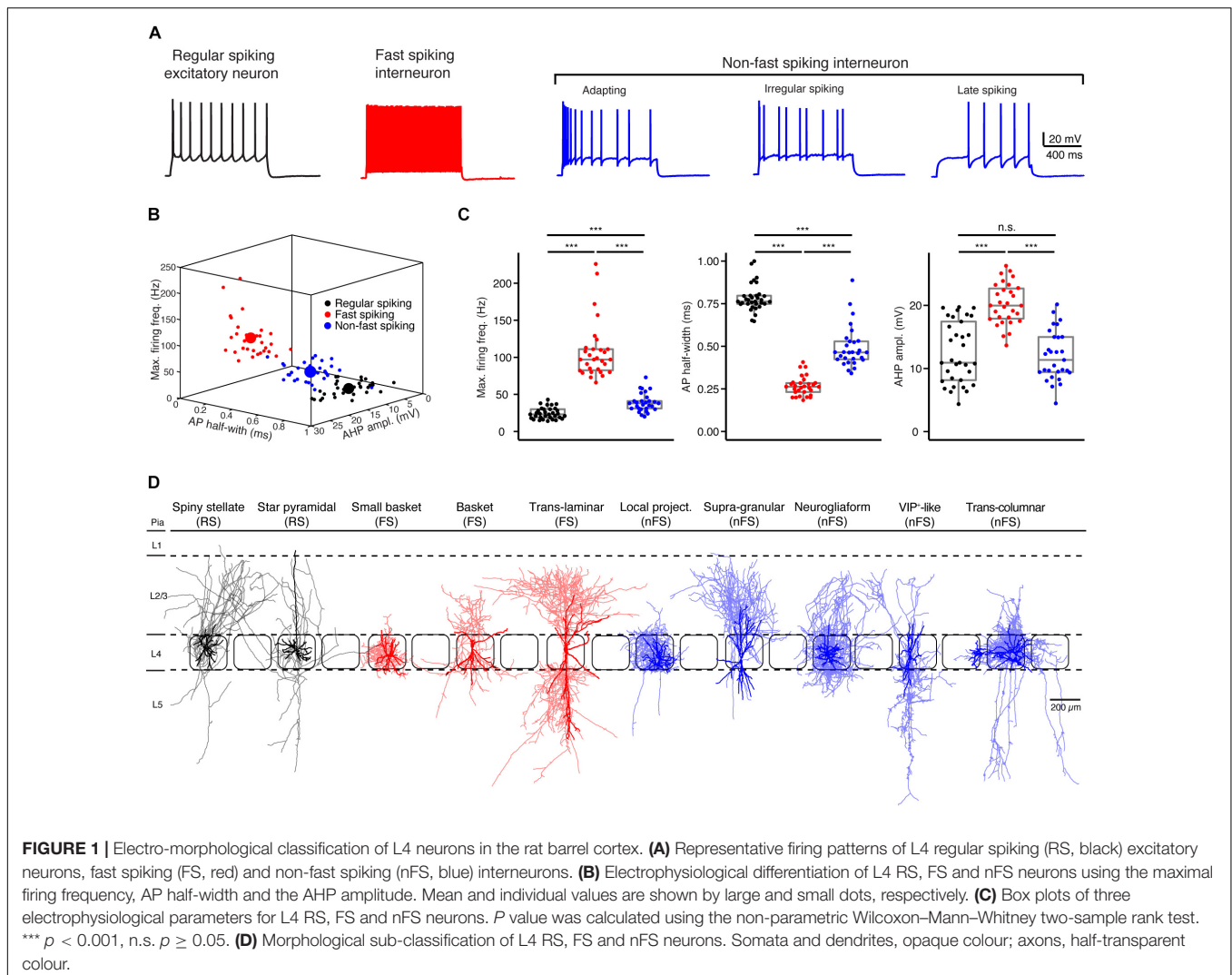
In addition to their electrophysiological diversity, L4 neurons show highly distinct dendritic and in particular axonal morphologies (Figure 1D). L4 excitatory neurons fall into two main groups, spiny stellate neurons (SSNs) without an obvious apical dendrite and star pyramidal cells (SPCs) (Feldmeyer et al., 1999; Lubke et al., 2000; but see Staiger et al., 2004). Their axons originate from the soma or the

initial part of one basal dendrite and project locally in layer 4 and to supra- and infragranular layers. Dendrites of L4 interneurons are aspiny or sparsely spiny and exhibit small to large multipolar, bipolar, or bitufted orientation patterns. Their axons project either locally in layer 4 and/or to supra- and/or infragranular layers in the vertical direction and/or to neighbouring columns in the horizontal direction. In previous studies, we have classified L4 FS interneurons as small basket cells (sBCs), basket cells (BCs), and translaminal cells (TLCs) (Koelbl et al., 2015) and L4 nFS interneurons as local-projecting (LP; non-Martinotti cell-like), supragranular-projecting (SP; Martinotti cell-like), neurogliaform (NGF), VIP+ -like (VIP) and transcolumar-projecting, interneurons (Emmenegger et al., 2018; Figure 1D).

Acetylcholine at Low Concentrations Induces Diverse Changes in the Membrane Potential of Layer 4 Neurons

We bath-applied 30 μ M ACh while monitoring changes in the V_m of L4 neurons under current-clamp conditions. Of 44 L4 RS neurons, 42 showed a hyperpolarisation; only two showed no change (Figures 2A,D). On average, ACh-induced V_m change in L4 RS neurons was -2.8 ± 1.4 mV ($n = 44$) (Figure 3A). Of 33 L4 FS interneurons, 25 neurons showed a weak but significant depolarisation of the V_m , four a weak hyperpolarisation and another four no change (Figures 2B,E). On average, the ACh application resulted in a change in V_m in L4 FS interneurons was 0.9 ± 1.5 mV ($n = 33$) (Figure 3A). Of 31 L4 nFS interneurons, 29 neurons showed a strong depolarisation of the V_m and two a hyperpolarisation (Figures 2C,F). For the majority of L4 nFS interneurons (25 out of 31), the ACh-induced depolarisation was subthreshold. In a small fraction of L4 nFS interneurons (4 out of 31), ACh application evoked a suprathreshold depolarisation so that spontaneous AP firing was initiated. On average, the ACh-induced change in V_m in L4 nFS interneurons was 5.2 ± 5.8 mV ($n = 31$) (Figure 3A). Note that the ACh-induced V_m changes were fully reversible by bath application of control ACSF (Figures 2A–C). To examine whether these ACh-induced changes in V_m resulted from a direct effect on the neuronal excitability or were caused indirectly by altering the activity of local synaptic microcircuits, a cocktail of synaptic blockers comprising CNQX (10 μ M), D-AP5 (50 μ M), and gabazine (10 μ M) was applied before ACh. There is no difference in the V_m change elicited by ACh in the absence and in the presence of synaptic blockers (Supplementary Figure 1). However, a clear decrease in background noise of V_m was observed in the presence of synaptic blockers (Supplementary Figure 1). A correlation analysis between the change in V_m and the age of the animal, V_{rest} and R_{in} demonstrated that there is no clear age-dependence of the ACh effect on V_m for any of the three L4 neuron types (Supplementary Figure 2A); a significant negative correlation was found between the V_m change and V_{rest} for L4 RS neurons ($r = -0.53$, $p = 1.8 \times 10^{-4}$) and L4 nFS interneurons ($r = -0.48$, $p = 5.9 \times 10^{-3}$) (Supplementary Figure 2B). Furthermore, for L4 nFS interneurons, a significant positive correlation was found

¹<https://huygens.science.uva.nl/PlotsOfData/>

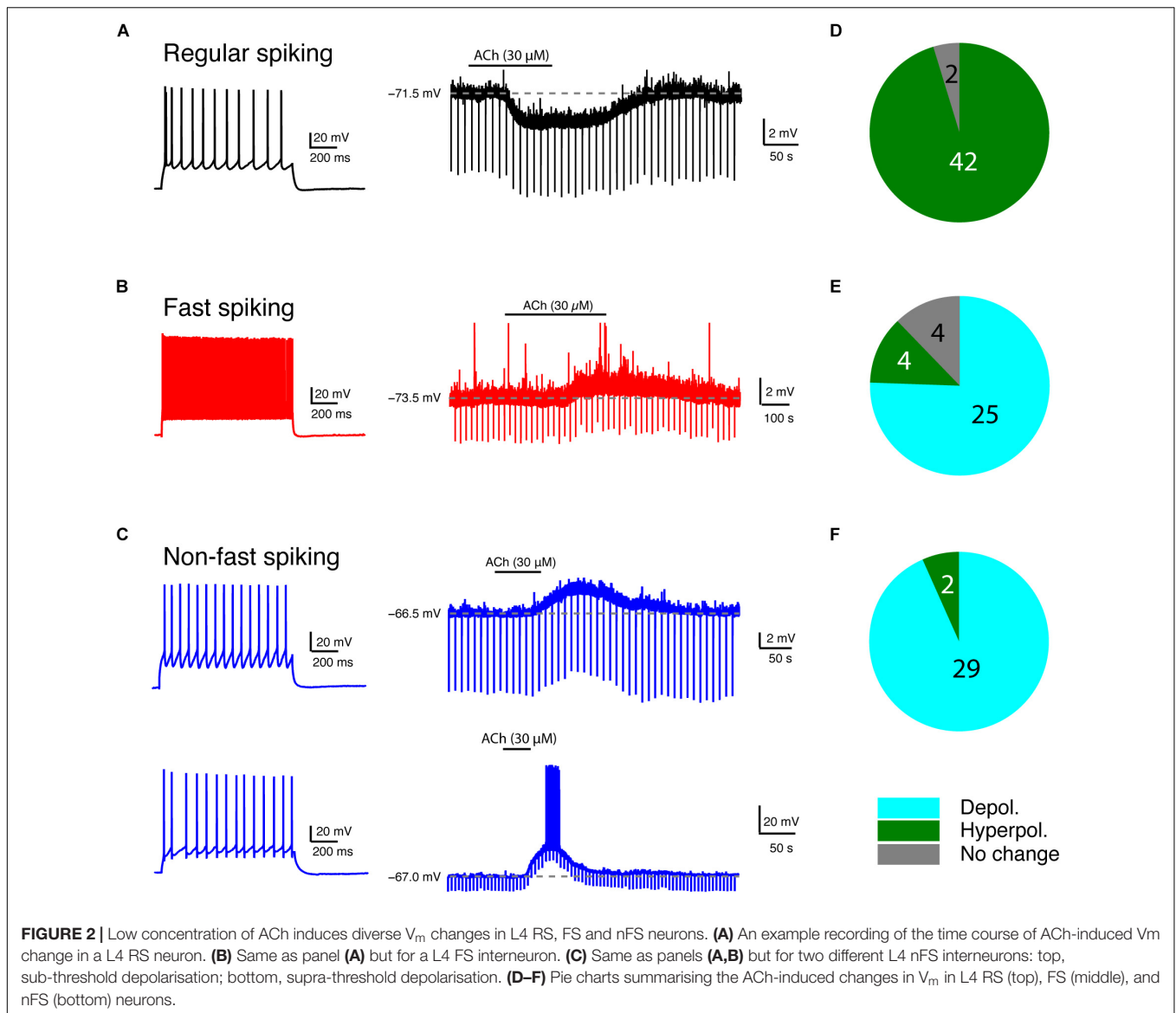


between the ACh-induced change in V_m and R_{in} ($r = 0.77$, $p = 1.6 \times 10^{-7}$; **Supplementary Figure 2C**), i.e., L4 nFS interneurons with higher R_{in} showed a larger depolarisation.

To evaluate the cell-type specificity of ACh-induced changes in V_m in more detail, we grouped the ACh response with respect to the L4 neuron subtype identified by the electrophysiological and morphological features described above. The two L4 RS excitatory neuron subtypes did not exhibit a significantly different ACh response (SSCs: -2.9 ± 1.4 mV, $n = 25$; SPNs: -2.8 ± 1.6 mV, $n = 19$; $p = 0.85$; **Figure 3B**). Similarly, no significant difference was found in the ACh-induced change in V_m among the three L4 FS interneuron subtypes (sBCs: 0.8 ± 1.0 mV, $n = 17$; BCs: 1.3 ± 2.3 mV, $n = 8$; TLCs: 0.5 ± 1.3 mV, $n = 8$; $p = 0.42$; **Figure 3C**). In contrast, in four subtypes of L4 nFS interneurons the ACh-induced V_m change in VIP interneurons was significantly larger than that in the other three subtypes (LPs: 3.0 ± 2.7 mV, $n = 9$; SPs: 3.8 ± 2.2 mV, $n = 11$; NGFs: 2.8 ± 0.5 mV, $n = 4$; VIPs: 14.3 ± 6.7 mV, $n = 6$; $p = 1.5 \times 10^{-3}$) (**Figure 3D**). We did not record the ACh response of the transcolumnar-projecting L4 nFS interneuron due to their scarcity.

Acetylcholine Differentially Changes the Intrinsic Excitability of Layer 4 Fast Spiking and Non-fast Spiking Interneurons

Acetylcholine not only modulates V_m but also induces changes in other intrinsic properties of L4 neurons. We have previously studied the effects of 100 μ M ACh on the intrinsic properties of L4 excitatory neurons (Eggermann and Feldmeyer, 2009) and demonstrated that ACh reduces their excitability through a hyperpolarisation of V_m and a reduction in R_{in} . In this study, we focussed mainly on L4 interneurons. Low concentrations of ACh (30 μ M) induced no significant change in the intrinsic properties of L4 FS interneurons except for the V_m (cf. **Figures 2, 3**). For example, no change was found for the AP half-width (Control: 0.26 ± 0.06 ms, $n = 8$; ACh: 0.26 ± 0.05 ms, $n = 8$; $p = 0.31$) and the AP amplitude (Control: 88.0 ± 12.6 mV, $n = 8$; ACh: 80.0 ± 8.9 mV, $n = 8$; $p = 0.08$) (**Figure 4A** and **Supplementary Table 1**). In contrast, apart from V_m changes (cf. **Figures 2, 3**) ACh also altered three other intrinsic electrophysiological



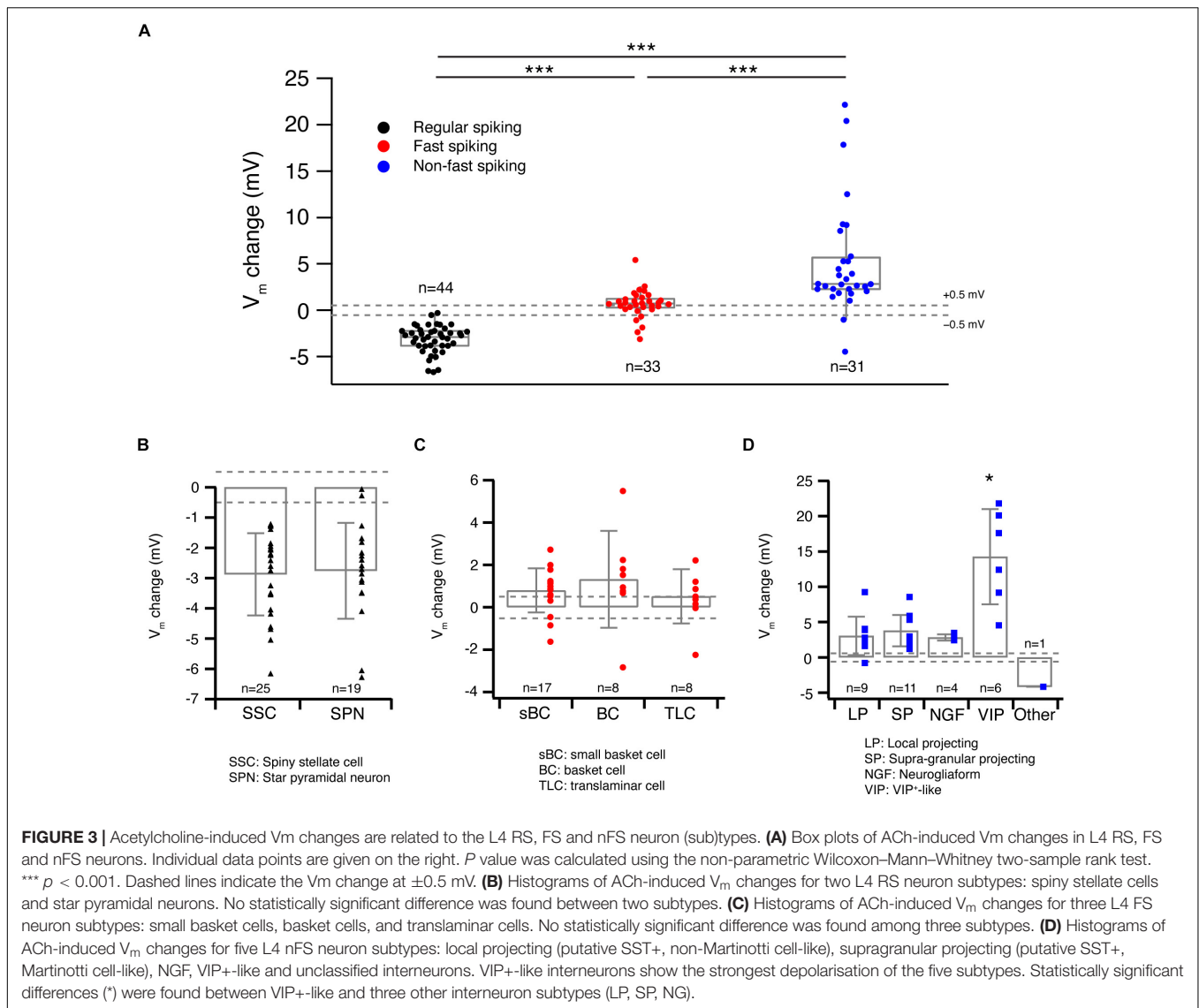
properties of L4 nFS interneurons: the AP half-width was increased (Control: 0.44 ± 0.10 ms, $n = 10$; ACh: 0.48 ± 0.11 ms, $n = 10$; $p = 0.04$) and the AP amplitude was decreased (Control: 92.8 ± 10.9 mV, $n = 10$; ACh: 82.6 ± 11.4 mV, $n = 10$; $p = 2.0 \times 10^{-3}$) (Figure 4B). Furthermore, the rheobase current was significantly reduced by ACh (Control: 158.08 ± 75.5 pA, $n = 10$; ACh: 84.0 ± 113.1 pA, $n = 10$; $p = 5.9 \times 10^{-3}$) (Supplementary Table 1). Thus, in contrast to L4 excitatory neurons, ACh enhanced the excitability of all recorded L4 nFS interneuron types.

One particular L4 nFS interneuron (Figure 4C) responded to ACh application with a V_m hyperpolarisation, in contrast to most L4 nFS interneurons. Furthermore, ACh changed its repetitive firing property (Figure 4C). Under control condition, this neuron showed a regular spiking firing pattern with a small spike-frequency adaptation, which in the presence of $30 \mu\text{M}$ ACh was transformed to an accelerating firing pattern

together with a spike amplitude accommodation. In addition, AP firing persisted even after terminating current injection. Because firing pattern and V_m returned to normal after washout (Figure 4C), the marked alteration in the firing pattern cannot be the result of deteriorating recording conditions. Hence, already at low concentrations, ACh can dramatically change the electrophysiological behaviour of a subpopulation of L4 nFS interneurons.

Acetylcholine-Induced Membrane Potential Changes in Layer 4 Neurons Are Mainly Regulated by Muscarinic Receptors

To reveal the molecular mechanism of ACh-induced V_m changes in L4 neurons, slices were superfused with the general mAChR antagonist ATRO (200 nM) before application of

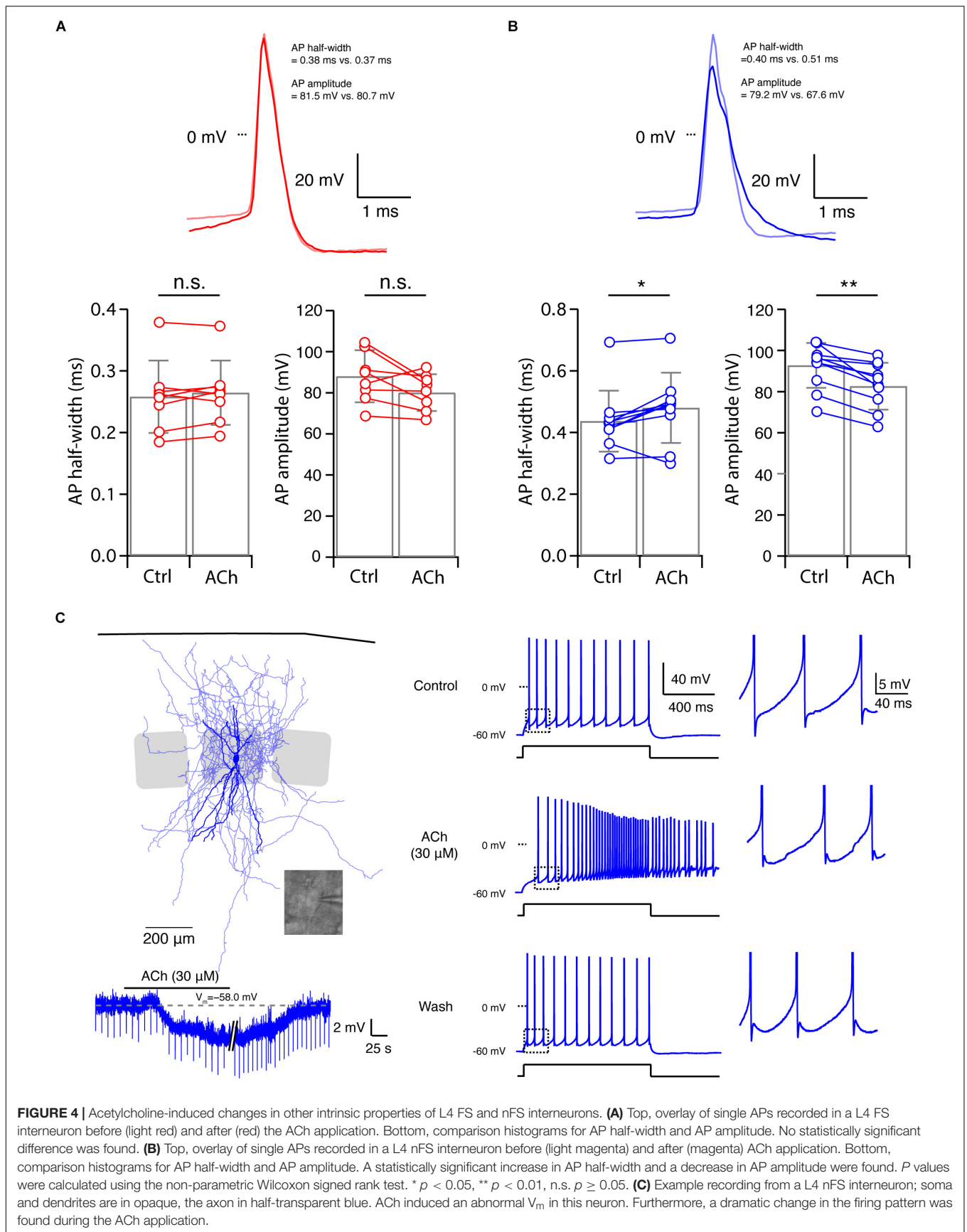


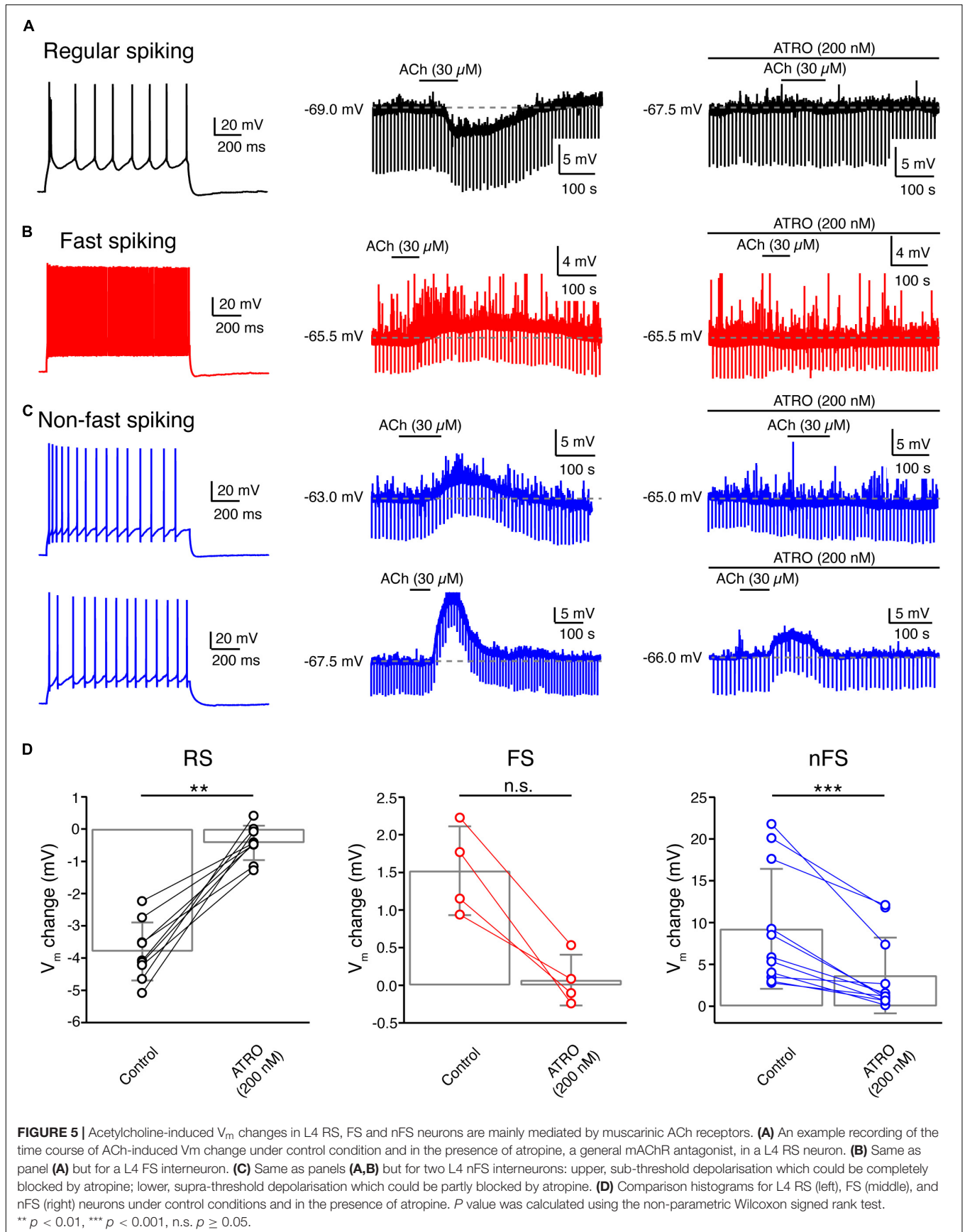
ACh. A comparison of the ACh-induced change in V_m before and during co-application of ATRO showed that the mAChR antagonist completely blocked the response in all L4 RS excitatory neurons (Control: -3.8 ± 0.9 mV, $n = 9$; ATRO: -0.4 ± 0.5 mV, $n = 9$; $p = 3.9 \times 10^{-3}$) (Figures 5A,D) and all L4 FS interneurons (Control: 1.5 ± 0.6 mV, $n = 4$; ATRO: 0.1 ± 0.3 mV, $n = 4$; $p = 0.13$) (Figures 5B,D). This suggests that the ACh-induced V_m changes in these L4 neuron types are exclusively mediated by mAChRs. In contrast, in L4 nFS interneurons, ATRO largely (but not completely) blocked the V_m change induced by $30 \mu\text{M}$ ACh (Control: 9.2 ± 7.2 mV, $n = 11$; ATRO: 3.7 ± 4.5 mV, $n = 11$; $p = 9.8 \times 10^{-4}$) (Figures 5C,D). In the majority (8 out of 11) of L4 nFS interneurons, ATRO nearly completely blocked the ACh-induced V_m change while in the remainder (3 out of 11), a residual ACh-induced change in V_m still persisted after the co-application of ATRO. We tested whether this residual depolarisation was mediated by nAChRs (see below). To identify the mAChR type mediating the modulatory effect, TRO ($1 \mu\text{M}$),

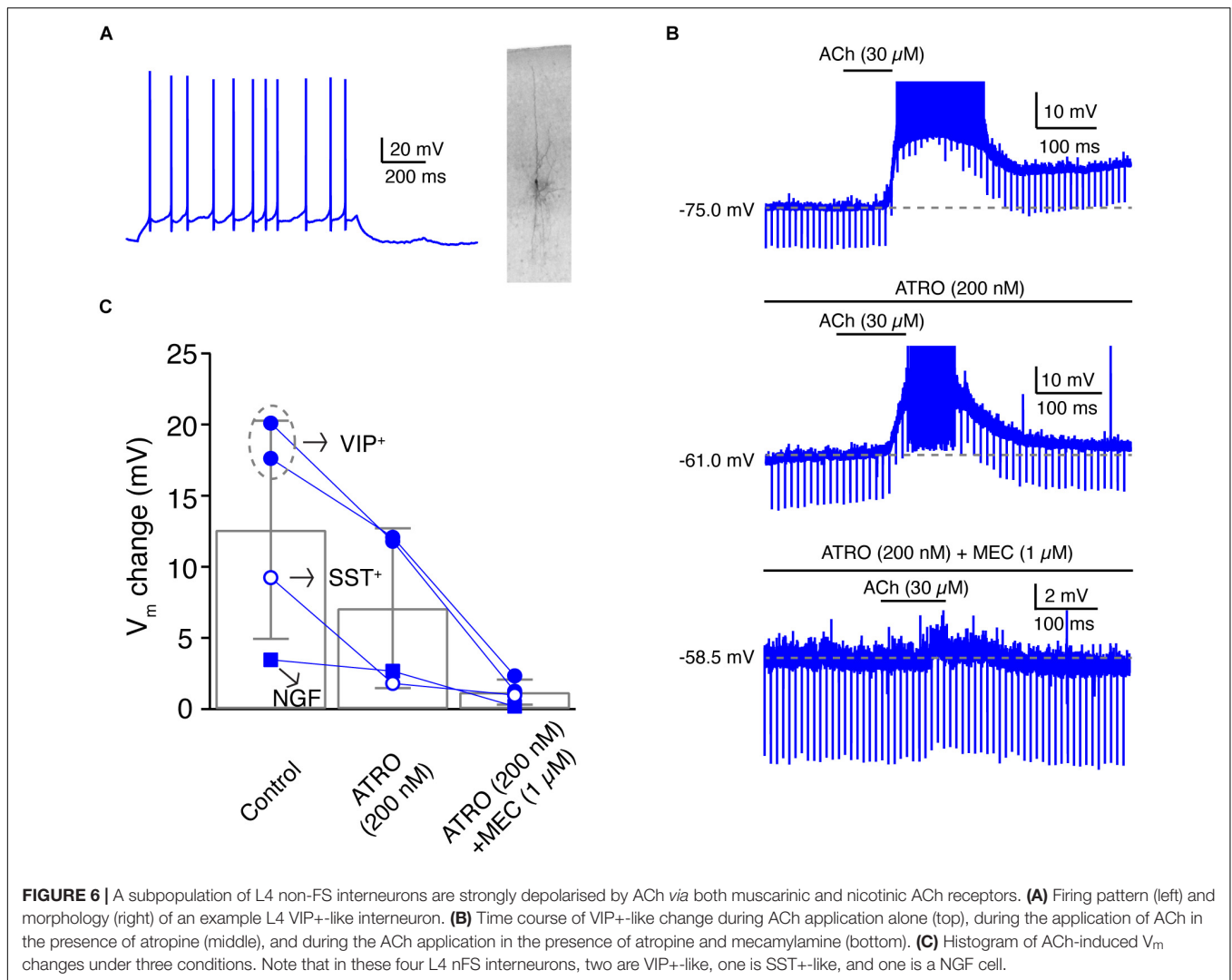
a specific M4 mAChR antagonist, and PIR ($0.5 \mu\text{M}$), a specific M1 mAChR antagonist, were applied before ACh. We found that TRO completely blocked the ACh-induced hyperpolarisation in L4 RS excitatory neurons (Supplementary Figure 3A) while PIR completely blocked the ACh-induced depolarisation in L4 FS interneurons (Supplementary Figure 3B). However, in L4 nFS interneurons, PIR blocked the ACh-induced depolarisation only partially (Supplementary Figure 3C).

Layer 4 VIP+-Like Non-fast Spiking Interneurons Are Strongly Depolarised by Low-Concentration of Acetylcholine via Both Muscarinic and Nicotinic Receptors

The fact that a subset of L4 nFS interneurons showed a strong ACh-induced depolarisation (Figures 2C, 3A,D) that was not fully blocked by ATRO (Figures 5C,D) indicates that





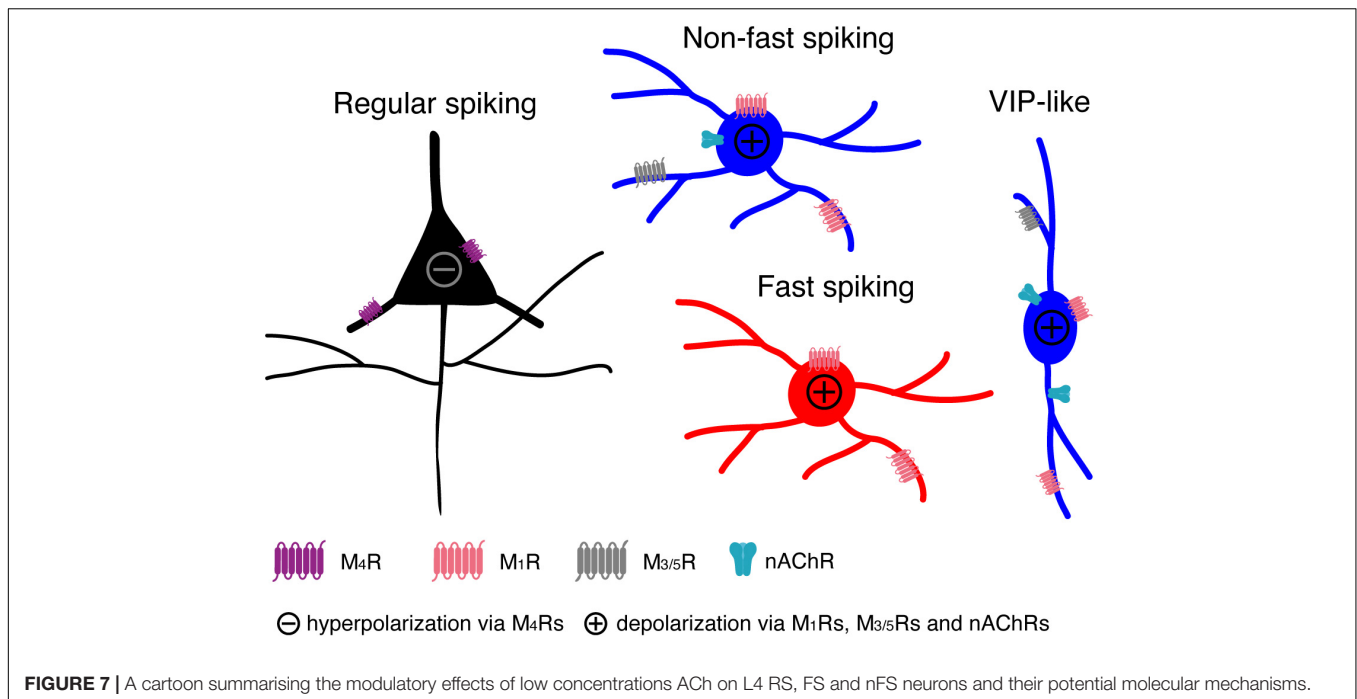


these interneurons may respond to ACh *via* both mAChRs and nAChRs. In those L4 nFS interneurons, in which ATRO blocked the ACh-induced depolarisation only incompletely, MEC (1 μ M), a general nAChR antagonist, together with ATRO were applied before ACh. An example recording from a putative L4 VIP+ nFS interneuron (Figure 6A) is shown in Figure 6B. This neuron exhibits an irregular firing pattern, a bipolar dendritic structure, and a narrow translaminal axonal projection, all of which are characteristics typical of VIP+ interneurons (Porter et al., 1998; Pronneke et al., 2015; Emmenegger et al., 2018). ACh induced a strong depolarisation in this neuron and elicited spontaneous AP firing. Even in the presence of ATRO, the ACh-induced AP firing still exists. Only when ATRO and MEC were applied together, was the ACh-induced change in V_m blocked (Figure 6B). A nAChR-mediated depolarisation was observed not only in L4 VIP+ interneurons ($n = 2$) but also in one putative SST+ interneuron and one NGF cell (Figure 6C). However, only VIP+ interneurons showed such a strong nAChR-mediated depolarisation. In one recording from a L4 VIP+ interneuron, we found that the ATRO-resistant depolarisation

was completely blocked by DH β E, a specific antagonist for $\alpha 4\beta 2$ -subunit containing nAChRs (Supplementary Figure 3C).

DISCUSSION

In the present study, we found that all L4 neuron types are persistently modulated by low concentrations of ACh in a cell-type specific way (see Figure 7): (1) ACh (30 μ M) reduces the intrinsic excitability of L4 RS excitatory neurons by activating the M4 mAChRs presumably located in the soma and/or dendrite, which leads to a hyperpolarisation of V_m and a decreased R_{in} ; (2) ACh induces a small but significant depolarisation in L4 FS interneurons by activating M1 mAChRs; (3) ACh elicits a markedly stronger depolarisation in L4 nFS interneurons compared to L4 FS interneurons by activating not only mAChRs (of the M1 and/or M3/5 type) but also nAChRs (presumably of the $\alpha 4\beta 2^*$ type); (4) In a subset of L4 nFS interneurons, the VIP+ -like interneurons, the ACh-induced depolarisation was sufficiently large to induce



spontaneous AP firing through activation of both mAChRs and nAChRs.

Layer 4 Neuronal Cell-Type Classification

A detailed neuronal cell-type classification is necessary and critical for an in-depth understanding the modulatory effects of ACh. Traditionally, neurons are classified based on their morphological (dendritic and axonal) and electrophysiological (repetitive firing) properties (Petilla Interneuron Nomenclature Group et al., 2008; DeFelipe et al., 2013). With the development and sophistication of single-cell mRNA sequencing techniques, the molecular features of neurons add an additional layer of complexity to neuronal classification (Zeng and Sanes, 2017; Yuste et al., 2020). We have performed a series of studies to dissect the neuronal diversity in layer 4 of rat barrel cortex (Feldmeyer et al., 1999; Lubke et al., 2000; Koelbl et al., 2015; Emmenegger et al., 2018). In general, layer 4 comprises three neuronal cell classes showing distinct repetitive firing properties: regular spiking, fast spiking and non-fast spiking (adapting, irregular, late, etc.). Taking the morphological diversity also into account, L4 RS excitatory neurons have been classified into spiny stellate cells and star pyramidal neurons (Feldmeyer et al., 1999; Lubke et al., 2000) while L4 FS interneurons have been divided into cluster 3 (small basket cells), cluster 2 (basket cells), and translamina-projecting FS interneurons (Koelbl et al., 2015). Most of these L4 FS interneurons are parvalbumin-positive (PV+) but calbindin-negative. L4 nFS interneurons, on the other hand, have been separated into five morpho-electrophysiological subtypes including transcolumar-projecting interneurons with an adapting firing pattern, locally projecting with an adapting firing pattern (presumably non-Martinotti cells), supragranular-projecting with an adapting

firing pattern with a Martinotti-cell appearance, VIP+ cell-like with an irregular firing pattern (VIP+-like) and neurogliaform cells (Emmenegger et al., 2018). The former three subtypes are somatostatin-positive while the latter two Prox1-positive. Our classification of L4 neurons is in line with several other groups focusing on the barrel cortex or primary visual cortex of rats and mice (Gibson et al., 1999; Porter et al., 2001; Beierlein et al., 2003; Ma et al., 2006; Scala et al., 2019).

The Necessity of Bath-Application of Low-Concentration Acetylcholine to Study the Tonic Neuromodulation Mediated by Muscarinic Receptors

Previously, it has been shown that the ACh concentration in the cerebrospinal fluid is in a low micromolar range, which fluctuates between 1 and 10 μM depending on the brain state (Himmelheber et al., 2000; Mattinson et al., 2011; Teles-Griolo Ruivo et al., 2017). Recently, accumulating evidence indicates that functional synaptic contacts are also established by cholinergic afferents in the neocortex. ACh is released into the synaptic cleft and its concentration can reach a very high concentration ($> 1 \text{ mM}$) (Turrini et al., 2001; Bennett et al., 2012; Hay et al., 2016; Obermayer et al., 2019). However, the exact extracellular concentration of ACh is still under investigation due to the species differences and difficulties arising from the rapid breakdown by acetylcholinesterase. ACh modulates the intrinsic neuronal properties through both mAChRs and nAChRs. mAChRs are G-protein coupled receptors the activation of which initiates a signalling cascade inside the neuron. In contrast, nAChRs form ligand-gated cation channels (Unwin, 2003; Dani, 2015). These two types of receptors work at

different concentrations of ACh. mAChRs already show a high affinity to ACh at low concentrations (in the range of 1–100 μM) while nAChRs require a high concentration of ACh for maximal activity (in the mM range). Previous studies have used puff-application of 1–10 mM ACh to study the nicotinic effects of ACh on excitatory and inhibitory neurons in several cortical areas (Xiang et al., 1998; Gullledge and Stuart, 2005; Gullledge et al., 2007; Poorthuis et al., 2013a,b). Puff-application of agonists has a high spatiotemporal resolution and is therefore a suitable strategy to simulate phasic ACh release at cholinergic presynaptic terminals; it is also required to minimise the effects of nAChR desensitisation. In addition, at such high concentrations, ACh will not be hydrolysed (and hence inactivated) immediately so that it may persist at low concentrations in the perisynaptic space. Bath application of cholinergic agonists such as ACh and carbachol is a good approach to simulate the latter condition because the agonist concentration will be maintained at a constant level to allow the measurement of neuronal properties at equilibrium. Carbachol shares both the muscarinic and nicotinic actions of ACh but shows a slower binding, dissociation and desensitisation kinetics, in particular at nAChRs. In addition, carbachol is not degraded by acetylcholinesterase. Carbachol is not the natural agonist and the relative affinity of carbachol for mAChRs and nAChRs is likely to be different from that of ACh so that we may observe an activation of nAChRs with low concentrations of carbachol but not with ACh. In order to simulate the *in situ* action of cholinergic agonists, the natural agonist ACh has been used instead of carbachol in this study. It is likely that in the extracellular space, a neurotransmitter/neuromodulator is only present at a μM concentration because of its rapid diffusion from the synaptic release site (Borrotto-Escuela et al., 2015). In addition, application of high concentrations of ACh will mask the effects mediated by mAChRs so that the application of low concentrations ($\sim\mu\text{M}$) of ACh is a prerequisite to uncover their functional effects.

Unique Cholinergic Modulation of Layer 4 Excitatory Neurons

We have shown previously that 100 μM ACh persistently hyperpolarises L4 excitatory neurons and reduces their intrinsic excitability (Eggermann and Feldmeyer, 2009), an ACh effect markedly different from that observed in most of pyramidal cells except for L6A corticocortical neurons (Yang et al., 2020). In L2/3, L5 and corticothalamic L6A pyramidal cells, ACh induces a persistent depolarisation and therefore enhances the excitability.

The ACh-induced hyperpolarisation in L4 excitatory neurons is mediated exclusively by M4 mAChRs, a finding that is supported by another study using optogenetic activation of synaptic ACh release (Dasgupta et al., 2018). Here, using a lower concentration of ACh (30 μM), similar results were obtained. Note that, as discussed above, 30 μM is an ACh concentration closer to the physiological range than 100 μM . There was no clear difference between the ACh-induced hyperpolarisation in both L4 RS neuron subtypes suggesting that SSNs and SPCs express the same mAChR subtype at a similar density.

Acetylcholine Persistently Depolarises Layer 4 Fast Spiking Interneurons

The effects of ACh on FS interneurons have been a long-standing matter of debate. Conflicting results have been published by different research groups. Puff-application of 5 mM ACh induced a transient hyperpolarisation that was mediated by mAChRs in rat neocortical L5 FS interneurons (Xiang et al., 1998). Recently, in the mouse visual cortex it has been shown that optogenetically stimulated ACh release led to an indirect inhibition in L2/3 FS interneurons *via* “facilitation” of the cholinergic responses in L2/3 somatostatin-positive interneurons (Chen et al., 2015). On the other hand it has been postulated that ACh does not affect the V_m of FS interneurons. In the rat frontal cortex, bath-application of carbachol (10 μM) had no effect on L2/3 FS interneurons (Kawaguchi, 1997). In a follow-up study the same group used focal application of ACh (100 μM or 5 mM for comparison with the study by Xiang et al., 1998) onto FS interneurons in rat visual and prefrontal cortex; the authors concluded that the focal application itself (i.e., a mechanical artefact but not the transient ACh exposure) caused the hyperpolarising response (Gullledge et al., 2007). Except for Xiang et al. (1998), most investigators have been unable to show a direct effect of ACh on FS interneurons (Muñoz and Rudy, 2014); however, they reported a presynaptic effect of ACh. In contrast to previous studies, we found a persistent ACh-induced V_m depolarisation in L4 FS interneurons, an effect that appeared in all three subtypes of L4 FS interneurons. To the best of our knowledge, this is the first time that a direct depolarising effect of ACh on FS interneurons has been demonstrated conclusively. In addition, we were able to show that this effect is mediated by M1 mAChRs. The ACh-induced depolarisation persisted in the presence of GABA and glutamate receptor antagonists so that indirect effects of ACh can be excluded. We were unable to investigate the effect of ACh on another subtype of FS interneurons, the chandelier or axo-axonic cells, which are very scarce if not absent in cortical layer 4 (Wang et al., 2019).

Acetylcholine Modulates Layer 4 Non-fast Spiking Interneuron Activity in a Subtype-Specific Way

Layer 4 nFS interneurons are a heterogenous population with diverse firing patterns, dendritic/axonal morphologies and molecular expression patterns. To elucidate modulatory effects of ACh on L4 nFS interneurons, a clear separation into identifiable subtypes is required. The local- and supragranular-projecting subtypes of L4 nFS interneurons display an adapting firing pattern similar to that of somatostatin-positive interneurons. Indeed, immunocytochemistry revealed that both subtypes of L4 nFS interneurons are somatostatin-positive (Emmenegger et al., 2018). Here, we found that L4 SST+-like interneurons including both local projecting (non-Martinotti-like) and supragranular projecting (Martinotti-like) cells that responded to ACh with a strong depolarisation that is predominantly mediated by mAChRs. Consistent with our findings, in the mouse barrel cortex it has been shown that L4 SST+ interneurons were depolarised and fired spikes in response to bath-applied

muscarine (3 μM) (Xu et al., 2013). In one L4 SST+ -like interneuron, ACh induced a depolarisation mediated by both mAChRs and nAChRs suggesting that even at μM ACh concentrations activation of nAChRs may be also possible. In a previous study, it has been shown that ACh directly excites SST+ neurons *via* both mAChRs and nAChRs in layer 2/3 of mouse visual cortex (Chen et al., 2015). However, a very high concentration of ACh (10 mM) was puff-applied in that study, which is very different from the bath-application of ACh (30 μM) described here.

Excitation of VIP+ interneurons by nAChRs has been observed in several cortical areas of both rat and mouse (Porter et al., 1999; F  rezou et al., 2007; Koukouli et al., 2017; Askew et al., 2019; Pr  nneke et al., 2020). In the rat motor cortex, local pressure application of ACh (100 μM) or the selective nAChR agonist DMPP (100–500 mM) depolarised VIP+ interneurons located in layer 3–5 and induced a discharge of action potentials (Porter et al., 1999). Pharmacological experiments suggested that the ACh effect was mediated by non- $\alpha 7$ nicotinic receptors containing $\alpha 4\beta 2$ and $\alpha 5$ subunits (Koukouli et al., 2017). In another study from the same group, it has been shown that bath-application of nicotine (1 μM) also resulted in a strong depolarisation leading to a sustained action potential discharge in VIP+ interneurons (F  rezou et al., 2007). Similarly, bath-application of nicotine (1 μM) in the mouse auditory cortex caused sustained AP discharge in VIP+ interneurons across the layers (Askew et al., 2019). In the mouse barrel cortex, bath-application of ACh (40 μM) efficiently depolarised L2/3 VIP+ interneurons and changed the firing pattern from bursting to tonic spiking in a subpopulation (Pr  nneke et al., 2020); however, the authors concluded that cholinergic modulation was mediated exclusively by nAChRs. All of the aforementioned studies emphasised the critical role of nAChRs in the cholinergic modulation of VIP+ interneurons but overlooked any direct involvement of mAChRs. However, our recordings from L4 VIP+ interneurons demonstrated that both AChR subtypes participate in the cholinergic modulation in a cooperative way because ATRO partially blocked the depolarisation or shortened the duration of repetitive AP firing induced by ACh; ATRO together with the nAChR antagonist MEC completely blocked the ACh effect. Similarly, in rat frontal cortex, VIP+ cells showed a sustained V_m depolarisation in response to bath-applied muscarine (3 μM) in the presence of TTX (Kawaguchi, 1997) indicating that mAChRs are expressed in these interneurons.

For NGF cells, the focus of attention is mostly cortical layer 1 where NGF cells are abundant (Christophe et al., 2002; Gullledge et al., 2007; Arroyo et al., 2012; Brombas et al., 2014). Puff-application of nicotinic agonists such as ACh, DMPP, choline onto L1 NGF cells or optogenetic stimulation of cholinergic fibres in layer 1 has revealed nicotinic excitation of NGF cells. Similar results have been shown for L2/3 5-HT_{3a}R+ NGF cells of mouse barrel cortex (Lee et al., 2010). Here, we found that in L4 NGF cells of the barrel cortex, low concentrations of ACh led to a mAChR-mediated sustained depolarisation. In one L4 NGF cell, a participation of nAChRs in this depolarisation was also found.

In addition to SST+, VIP+, and NGF cells, layer 4 comprises other nFS subtypes (Tasic et al., 2018). In one L4 nFS interneuron, we were able to show that, in contrast to most other L4 nFS interneurons, ACh application resulted in a hyperpolarisation of this neuron and dramatically changed its repetitive firing pattern during the suprathreshold current injection. The cholinergic response of this neuron together with its firing pattern and morphology, is reminiscent of a subset of CCK+ neurons in L2/3 of rat frontal cortex which exhibited a prominent hyperpolarisation in response to muscarine (3 μM) and had large somata and an extensive axonal arbour (Kawaguchi, 1997). Therefore, the nFS interneuron showing an ACh-induced hyperpolarisation described here could be a L4 CCK+ neuron. Similarly, some hippocampal CA1 CCK+ interneurons showed also an ACh-induced hyperpolarisation mediated by mAChRs (McQuiston and Madison, 1999b; Cea-del Rio et al., 2011). Furthermore, the dramatic change in firing pattern induced by ACh has also been demonstrated in hippocampal CA1 CCK+ interneurons (McQuiston and Madison, 1999a; Lawrence et al., 2006; Cea-del Rio et al., 2010, 2011). In these neurons, through the activation of M1 and M3 mAChRs the AHP was superimposed by an afterdepolarisation which is often sufficiently strong to evoke APs in the absence of further stimulation (McQuiston and Madison, 1999a; Cea-del Rio et al., 2011).

Functional Significance of Cholinergic Neuromodulation for Layer 4 Neuronal Microcircuits

In the neocortex, ACh is continuously released into the extracellular space and its level changes dramatically during the animal's diurnal cycle and different behavioural states (Teles-Grilo Ruivo et al., 2017). Furthermore, there is increasing evidence for changes in ACh receptor expression levels going hand in hand with the diurnal change in ACh drive (Hut and Van der Zee, 2011). Most of the intracortical ACh is not released at synaptic contacts but rather diffusely into the extracellular space through an extrasynaptic volume transmission (Fuxe and Borroto-Escuela, 2016). Under this condition, cholinergic modulation is spatiotemporally slower but broader, thereby tuning neuronal network function. Modulation of neurons and their synaptic interactions through mAChRs may induce neuronal oscillations and therefore change the information processing mode in L4 neuronal microcircuits. Specifically, cholinergic activation of L4 FS, PV+, and nFS, SST+ interneurons by low concentrations of ACh may lead to the generation of persistent activity such as the gamma rhythm, which has been demonstrated to enhance the cortical circuit performance (Bartos et al., 2007; Sohal et al., 2009; Veit et al., 2017). Indeed, it has been demonstrated that bath-application of carbachol (10 μM) to activate mAChRs and kainate (300 nM) to increase the tonic excitatory drive elicited persistent gamma frequency network oscillations in cortical layer 4 of mouse barrel cortex (Buhl et al., 1998). In addition, differential modulation of L4 excitatory and inhibitory neurons, i.e., the persistent hyperpolarisation of L4 excitatory neurons and depolarisation of most L4 inhibitory neurons, will change the excitation-inhibition

balance towards inhibition and reduce the responsiveness of the L4 recurrent excitatory microcircuit. Therefore, our results support the hypothesis that ACh has a filtering action in the major recipient layer of the neocortex (Eggermann and Feldmeyer, 2009). Because neocortical layer 4 is uniquely positioned to gate thalamocortical input to the neocortex, cholinergic modulation of L4 neuronal microcircuits will affect the whole barrel cortex together with the related cortical areas (e.g., M1 and S2) and finally the animal behaviour (Eggermann et al., 2014; Meir et al., 2018). In addition, our finding that mAChRs ubiquitously but differentially modulate the activity of L4 excitatory and inhibitory neurons might open the door to more specific therapeutic strategies to treat cognitive dysfunction or psychiatric disorders linked to degeneration of the cholinergic system in diseases such as Alzheimer's disease and schizophrenia (Marin, 2012; Hampel et al., 2018).

DATA AVAILABILITY STATEMENT

The original contributions presented in the study are included in the article/**Supplementary Material**, further inquiries can be directed to the corresponding authors.

ETHICS STATEMENT

All experimental procedures involving animals were performed in accordance with the guidelines of the Federation of European Laboratory Animal Science Association (FELASA), the EU Directive 2010/63/EU, and the German animal welfare law.

REFERENCES

- Arroyo, S., Bennett, C., Aziz, D., Brown, S. P., and Hestrin, S. (2012). Prolonged disynaptic inhibition in the cortex mediated by slow, non- $\alpha 7$ nicotinic excitation of a specific subset of cortical interneurons. *J. Neurosci.* 32, 3859–3864. doi: 10.1523/jneurosci.0115-12.2012
- Askew, C. E., Lopez, A. J., Wood, M. A., and Metherate, R. (2019). Nicotine excites VIP interneurons to disinhibit pyramidal neurons in auditory cortex. *Synapse* 73:e22116. doi: 10.1002/syn.22116
- Bacci, A., Huguenard, J. R., and Prince, D. A. (2005). Modulation of neocortical interneurons: extrinsic influences and exercises in self-control. *Trends Neurosci.* 28, 602–610. doi: 10.1016/j.tins.2005.08.007
- Bailey, C. D., De Biasi, M., Fletcher, P. J., and Lambe, E. K. (2010). The nicotinic acetylcholine receptor $\alpha 5$ subunit plays a key role in attention circuitry and accuracy. *J. Neurosci.* 30, 9241–9252. doi: 10.1523/JNEUROSCI.2258-10.2010
- Bartos, M., Vida, I., and Jonas, P. (2007). Synaptic mechanisms of synchronized gamma oscillations in inhibitory interneuron networks. *Nat. Rev. Neurosci.* 8, 45–56. doi: 10.1038/nrn2044
- Beierlein, M., Gibson, J. R., and Connors, B. W. (2003). Two dynamically distinct inhibitory networks in layer 4 of the neocortex. *J. Neurophysiol.* 90, 2987–3000. doi: 10.1152/jn.00283.2003
- Bennett, C., Arroyo, S., Berns, D., and Hestrin, S. (2012). Mechanisms generating dual-component nicotinic EPSCs in cortical interneurons. *J. Neurosci.* 32, 17287–17296. doi: 10.1523/jneurosci.3565-12.2012
- Borroto-Escuela, D. O., Agnati, L. F., Bechter, K., Jansson, A., Tarakanov, A. O., and Fuxe, K. (2015). The role of transmitter diffusion and flow versus extracellular vesicles in volume transmission in the brain neural-glia networks. *Philos. Trans. R. Soc. Lond. B Biol. Sci.* 370:0183. doi: 10.1098/rstb.2014.0183
- Brombas, A., Fletcher, L. N., and Williams, S. R. (2014). Activity-dependent modulation of layer 1 inhibitory neocortical circuits by acetylcholine. *J. Neurosci.* 34, 1932–1941. doi: 10.1523/jneurosci.4470-13.2014
- Buhl, E. H., Tamás, G., and Fisahn, A. (1998). Cholinergic activation and tonic excitation induce persistent gamma oscillations in mouse somatosensory cortex *in vitro*. *J. Physiol.* 513(Pt 1), 117–126. doi: 10.1111/j.1469-7793.1998.117by.x
- Cea-del Rio, C. A., Lawrence, J. J., Erdelyi, F., Szabo, G., and McBain, C. J. (2011). Cholinergic modulation amplifies the intrinsic oscillatory properties of CA1 hippocampal cholecystokinin-positive interneurons. *J. Physiol.* 589, 609–627. doi: 10.1113/jphysiol.2010.199422
- Cea-del Rio, C. A., Lawrence, J. J., Tricoire, L., Erdelyi, F., Szabo, G., and McBain, C. J. (2010). M3 muscarinic acetylcholine receptor expression confers differential cholinergic modulation to neurochemically distinct hippocampal basket cell subtypes. *J. Neurosci.* 30, 6011–6024. doi: 10.1523/JNEUROSCI.5040-09.2010
- Chen, N., Sugihara, H., and Sur, M. (2015). An acetylcholine-activated microcircuit drives temporal dynamics of cortical activity. *Nat. Neurosci.* 18, 892–902. doi: 10.1038/nn.4002
- Christophe, E., Roebuck, A., Staiger, J. F., Lavery, D. J., Charpak, S., and Audinat, E. (2002). Two types of nicotinic receptors mediate an excitation of neocortical layer I interneurons. *J. Neurophysiol.* 88, 1318–1327. doi: 10.1152/jn.2002.88.3.1318
- Colangelo, C., Shichkova, P., Keller, D., Markram, H., and Ramaswamy, S. (2019). Cellular, Synaptic and Network Effects of Acetylcholine in the Neocortex. *Front. Neural Circuits* 13:24. doi: 10.3389/fncir.2019.00024
- Dani, J. A. (2015). Neuronal Nicotinic Acetylcholine Receptor Structure and Function and Response to Nicotine. *Int. Rev. Neurobiol.* 124, 3–19. doi: 10.1016/bs.irn.2015.07.001

AUTHOR CONTRIBUTIONS

GQ designed research, performed experiments, analysed data, and wrote the draft manuscript. DF supervised the work and wrote the manuscript. Both authors contributed to the article and approved the submitted version.

FUNDING

This work was supported by the Helmholtz Society, the DFG Research Group–BaCoFun (grant no. Fe471/4-2 to DF) and European Union's Horizon 2020 Research Innovation Programme (grant agreement no. 785907; HBP SGA2 to DF).

ACKNOWLEDGMENTS

We are grateful to Danqing Yang for insightful comments and suggestions on the manuscript. We thank Werner Hucko for excellent technical assistance and Karlijn van Aerde for custom-written macros in Igor Pro software. We also thank Vishalini Emmenegger for help with NeuroLucida reconstructions.

SUPPLEMENTARY MATERIAL

The Supplementary Material for this article can be found online at: <https://www.frontiersin.org/articles/10.3389/fncir.2022.843025/full#supplementary-material>

- Dasgupta, R., Seibt, F., and Beierlein, M. (2018). Synaptic Release of Acetylcholine Rapidly Suppresses Cortical Activity by Recruiting Muscarinic Receptors in Layer 4. *J. Neurosci.* 38, 5338–5350. doi: 10.1523/jneurosci.0566-18.2018
- DeFelipe, J., Lopez-Cruz, P. L., Benavides-Piccione, R., Bielza, C., Larranaga, P., Anderson, S., et al. (2013). New insights into the classification and nomenclature of cortical GABAergic interneurons. *Nat. Rev. Neurosci.* 14, 202–216. doi: 10.1038/nrn3444
- Eggermann, E., and Feldmeyer, D. (2009). Cholinergic filtering in the recurrent excitatory microcircuit of cortical layer 4. *Proc. Natl. Acad. Sci. U S A.* 106, 11753–11758. doi: 10.1073/pnas.0810062106
- Eggermann, E., Kremer, Y., Crochet, S., and Petersen, C. C. H. (2014). Cholinergic signals in mouse barrel cortex during active whisker sensing. *Cell Rep.* 9, 1654–1660. doi: 10.1016/j.celrep.2014.11.005
- Emmenegger, V., Qi, G., Wang, H., and Feldmeyer, D. (2018). Morphological and Functional Characterization of Non-fast-Spiking GABAergic Interneurons in Layer 4 Microcircuitry of Rat Barrel Cortex. *Cereb. Cortex* 28, 1439–1457. doi: 10.1093/cercor/bhx352
- Feldmeyer, D., Egger, V., Lubke, J., and Sakmann, B. (1999). Reliable synaptic connections between pairs of excitatory layer 4 neurones within a single 'barrel' of developing rat somatosensory cortex. *J. Physiol.* 521(Pt 1), 169–190. doi: 10.1111/j.1469-7793.1999.00169.x
- Férézou, I., Hill, E. L., Cauli, B., Gibelin, N., Kaneko, T., Rossier, J., et al. (2007). Extensive overlap of mu-opioid and nicotinic sensitivity in cortical interneurons. *Cereb. Cortex* 17, 1948–1957. doi: 10.1093/cercor/bhl104
- Fuxe, K., and Borroto-Escuela, D. O. (2016). Volume transmission and receptor-receptor interactions in heteroreceptor complexes: understanding the role of new concepts for brain communication. *Neural Regen. Res.* 11, 1220–1223. doi: 10.4103/1673-5374.189168
- Gibson, J. R., Beierlein, M., and Connors, B. W. (1999). Two networks of electrically coupled inhibitory neurons in neocortex. *Nature* 402, 75–79. doi: 10.1038/47035
- Granger, A. J., Wang, W., Robertson, K., El-Rifai, M., Zanella, A. F., Bistrong, K., et al. (2020). Cortical ChAT(+) neurons co-transmit acetylcholine and GABA in a target- and brain-region-specific manner. *Elife* 9:57749. doi: 10.7554/eLife.57749
- Gulledge, A. T., and Stuart, G. J. (2005). Cholinergic inhibition of neocortical pyramidal neurons. *J. Neurosci.* 25, 10308–10320. doi: 10.1523/jneurosci.2697-05.2005
- Gulledge, A. T., Park, S. B., Kawaguchi, Y., and Stuart, G. J. (2007). Heterogeneity of phasic cholinergic signaling in neocortical neurons. *J. Neurophysiol.* 97, 2215–2229. doi: 10.1152/jn.00493.2006
- Hampel, H., Mesulam, M. M., Cuellar, A. C., Farlow, M. R., Giacobini, E., Grossberg, G. T., et al. (2018). The cholinergic system in the pathophysiology and treatment of Alzheimer's disease. *Brain* 141, 1917–1933. doi: 10.1093/brain/awy132
- Hasselmo, M. E. (2006). The role of acetylcholine in learning and memory. *Curr. Opin. Neurobiol.* 16, 710–715. doi: 10.1016/j.conb.2006.09.002
- Hay, Y. A., Lambolze, B., and Tricoire, L. (2016). Nicotinic Transmission onto Layer 6 Cortical Neurons Relies on Synaptic Activation of Non- $\alpha 7$ Receptors. *Cereb. Cortex* 26, 2549–2562. doi: 10.1093/cercor/bhv085
- Himmelheber, A. M., Sarter, M., and Bruno, J. P. (2000). Increases in cortical acetylcholine release during sustained attention performance in rats. *Brain Res. Cogn. Brain Res.* 9, 313–325. doi: 10.1016/s0926-6410(00)00012-4
- Hut, R. A., and Van der Zee, E. A. (2011). The cholinergic system, circadian rhythmicity, and time memory. *Behav. Brain Res.* 221, 466–480. doi: 10.1016/j.bbr.2010.11.039
- Kawaguchi, Y. (1997). Selective cholinergic modulation of cortical GABAergic cell subtypes. *J. Neurophysiol.* 78, 1743–1747. doi: 10.1152/jn.1997.78.3.1743
- Koelbl, C., Helmstaedter, M., Lübke, J., and Feldmeyer, D. (2015). A barrel-related interneuron in layer 4 of rat somatosensory cortex with a high intrabarrel connectivity. *Cereb. Cortex* 25, 713–725. doi: 10.1093/cercor/bht263
- Koukoulis, F., Rooy, M., Tziotis, D., Sailor, K. A., O'Neill, H. C., Levenga, J., et al. (2017). Nicotine reverses hypofrontality in animal models of addiction and schizophrenia. *Nat. Med.* 23, 347–354. doi: 10.1038/nm.4274
- Kruglikov, I., and Rudy, B. (2008). Perisomatic GABA release and thalamocortical integration onto neocortical excitatory cells are regulated by neuromodulators. *Neuron* 58, 911–924. doi: 10.1016/j.neuron.2008.04.024
- Lawrence, J. J., Statland, J. M., Grinspan, Z. M., and McBain, C. J. (2006). Cell type-specific dependence of muscarinic signalling in mouse hippocampal stratum oriens interneurons. *J. Physiol.* 570, 595–610. doi: 10.1113/jphysiol.2005.100875
- Lee, S., Hjerling-Leffler, J., Zagha, E., Fishell, G., and Rudy, B. (2010). The largest group of superficial neocortical GABAergic interneurons expresses ionotropic serotonin receptors. *J. Neurosci.* 30, 16796–16808. doi: 10.1523/jneurosci.1869-10.2010
- Lubke, J., Egger, V., Sakmann, B., and Feldmeyer, D. (2000). Columnar organization of dendrites and axons of single and synaptically coupled excitatory spiny neurons in layer 4 of the rat barrel cortex. *J. Neurosci.* 20, 5300–5311. doi: 10.1523/JNEUROSCI.20-14-05300.2000
- Ma, Y., Hu, H., Berrebi, A. S., Mathers, P. H., and Agmon, A. (2006). Distinct subtypes of somatostatin-containing neocortical interneurons revealed in transgenic mice. *J. Neurosci.* 26, 5069–5082. doi: 10.1523/JNEUROSCI.0661-06.2006
- Marin, O. (2012). Interneuron dysfunction in psychiatric disorders. *Nat. Rev. Neurosci.* 13, 107–120. doi: 10.1038/nrn3155
- Marx, M., Gunter, R. H., Hucko, W., Radnikow, G., and Feldmeyer, D. (2012). Improved biocytin labeling and neuronal 3D reconstruction. *Nat. Protoc.* 7, 394–407. doi: 10.1038/nprot.2011.449
- Mattinson, C. E., Burmeister, J. J., Quintero, J. E., Pomerleau, F., Huettl, P., and Gerhardt, G. A. (2011). Tonic and phasic release of glutamate and acetylcholine neurotransmission in sub-regions of the rat prefrontal cortex using enzyme-based microelectrode arrays. *J. Neurosci. Methods* 202, 199–208. doi: 10.1016/j.jneumeth.2011.08.020
- McQuiston, A. R., and Madison, D. V. (1999a). Muscarinic receptor activity induces an afterdepolarization in a subpopulation of hippocampal CA1 interneurons. *J. Neurosci.* 19, 5703–5710. doi: 10.1523/JNEUROSCI.19-14-05703.1999
- McQuiston, A. R., and Madison, D. V. (1999b). Muscarinic receptor activity has multiple effects on the resting membrane potentials of CA1 hippocampal interneurons. *J. Neurosci.* 19, 5693–5702. doi: 10.1523/jneurosci.19-14-05693.1999
- Meir, I., Katz, Y., and Lampl, I. (2018). Membrane Potential Correlates of Network Decorrelation and Improved SNR by Cholinergic Activation in the Somatosensory Cortex. *J. Neurosci.* 38, 10692–10708. doi: 10.1523/jneurosci.1159-18.2018
- Mesulam, M. M., Mufson, E. J., Levey, A. I., and Wainer, B. H. (1983). Cholinergic innervation of cortex by the basal forebrain: cytochemistry and cortical connections of the septal area, diagonal band nuclei, nucleus basalis (substantia innominata), and hypothalamus in the rhesus monkey. *J. Comp. Neurol.* 214, 170–197. doi: 10.1002/cne.902140206
- Muñoz, W., and Rudy, B. (2014). Spatiotemporal specificity in cholinergic control of neocortical function. *Curr. Opin. Neurobiol.* 26, 149–160. doi: 10.1016/j.conb.2014.02.015
- Obermayer, J., Luchicchi, A., Heistek, T. S., de Kloet, S. F., Terra, H., Bruinsma, B., et al. (2019). Prefrontal cortical ChAT-VIP interneurons provide local excitation by cholinergic synaptic transmission and control attention. *Nat. Commun.* 10:5280. doi: 10.1038/s41467-019-13244-9
- Obermayer, J., Verhoog, M. B., Luchicchi, A., and Mansvelder, H. D. (2017). Cholinergic Modulation of Cortical Microcircuits Is Layer-Specific: Evidence from Rodent, Monkey and Human Brain. *Front. Neural Circuits* 11:100. doi: 10.3389/fncir.2017.00100
- Patel, A. V., Codeluppi, S. A., Ervin, K. S. J., St-Denis, M. B., Choleris, E., and Bailey, C. D. C. (2021). Developmental Age and Biological Sex Influence Muscarinic Receptor Function and Neuron Morphology within Layer VI of the Medial Prefrontal Cortex. *Cereb. Cortex* 2021:bh406. doi: 10.1093/cercor/bh406
- Petilla Interneuron Nomenclature Group, Ascoli, G. A., Alonso-Nanclares, L., Anderson, S. A., Barrionuevo, G., Benavides-Piccione, R., et al. (2008). Petilla terminology: nomenclature of features of GABAergic interneurons of the cerebral cortex. *Nat. Rev. Neurosci.* 9, 557–568. doi: 10.1038/nrn2402
- Picciotto, M. R., Higley, M. J., and Mineur, Y. S. (2012). Acetylcholine as a neuromodulator: cholinergic signaling shapes nervous system function and behavior. *Neuron* 76, 116–129. doi: 10.1016/j.neuron.2012.08.036
- Poorthuis, R. B., Bloem, B., Verhoog, M. B., and Mansvelder, H. D. (2013a). Layer-specific interference with cholinergic signaling in the prefrontal cortex by smoking concentrations of nicotine. *J. Neurosci.* 33, 4843–4853. doi: 10.1523/jneurosci.5012-12.2013

- Poorthuis, R. B., Bloem, B., Schak, B., Wester, J., de Kock, C. P., and Mansvelder, H. D. (2013b). Layer-specific modulation of the prefrontal cortex by nicotinic acetylcholine receptors. *Cereb. Cortex* 23, 148–161. doi: 10.1093/cercor/bhr390
- Porter, J. T., Cauli, B., Staiger, J. F., Lambolez, B., Rossier, J., and Audinat, E. (1998). Properties of bipolar VIPergic interneurons and their excitation by pyramidal neurons in the rat neocortex. *Eur. J. Neurosci.* 10, 3617–3628. doi: 10.1046/j.1460-9568.1998.00367.x
- Porter, J. T., Cauli, B., Tsuzuki, K., Lambolez, B., Rossier, J., and Audinat, E. (1999). Selective excitation of subtypes of neocortical interneurons by nicotinic receptors. *J. Neurosci.* 19, 5228–5235. doi: 10.1523/jneurosci.19-13-05228.1999
- Porter, J. T., Johnson, C. K., and Agmon, A. (2001). Diverse types of interneurons generate thalamus-evoked feedforward inhibition in the mouse barrel cortex. *J. Neurosci.* 21, 2699–2710. doi: 10.1523/JNEUROSCI.21-08-02699.2001
- Postma, M., and Goedhart, J. (2019). PlotsOfData—A web app for visualizing data together with their summaries. *PLoS Biol.* 7:e3000202. doi: 10.1371/journal.pbio.3000202
- Pronneke, A., Scheuer, B., Wagener, R. J., Mock, M., Witte, M., and Staiger, J. F. (2015). Characterizing VIP Neurons in the Barrel Cortex of VIPcre/tdTomato Mice Reveals Layer-Specific Differences. *Cereb. Cortex* 25, 4854–4868. doi: 10.1093/cercor/bhv202
- Prönneke, A., Witte, M., Möck, M., and Staiger, J. F. (2020). Neuromodulation Leads to a Burst-Tonic Switch in a Subset of VIP Neurons in Mouse Primary Somatosensory (Barrel) Cortex. *Cereb. Cortex* 30, 488–504. doi: 10.1093/cercor/bhz102
- Qi, G., van Aerde, K., Abel, T., and Feldmeyer, D. (2017). Adenosine Differentially Modulates Synaptic Transmission of Excitatory and Inhibitory Microcircuits in Layer 4 of Rat Barrel Cortex. *Cereb. Cortex* 27, 4411–4422. doi: 10.1093/cercor/bhw243
- Radnikow, G., and Feldmeyer, D. (2018). Layer- and Cell Type-Specific Modulation of Excitatory Neuronal Activity in the Neocortex. *Front. Neuroanat.* 12:1. doi: 10.3389/fnana.2018.00001
- Scala, F., Kobak, D., Shan, S., Bernaerts, Y., Laternus, S., Cadwell, C. R., et al. (2019). Layer 4 of mouse neocortex differs in cell types and circuit organization between sensory areas. *Nat. Commun.* 10:4174. doi: 10.1038/s41467-019-12058-z
- Sohal, V. S., Zhang, F., Yizhar, O., and Deisseroth, K. (2009). Parvalbumin neurons and gamma rhythms enhance cortical circuit performance. *Nature* 459, 698–702. doi: 10.1038/nature07991
- Staiger, J. F., Flagmeyer, I., Schubert, D., Zilles, K., Kotter, R., and Luhmann, H. J. (2004). Functional diversity of layer IV spiny neurons in rat somatosensory cortex: quantitative morphology of electrophysiologically characterized and biocytin labeled cells. *Cereb. Cortex* 14, 690–701. doi: 10.1093/cercor/bhh029
- Tasic, B., Yao, Z., Graybiel, L. T., Smith, K. A., Nguyen, T. N., Bertagnolli, D., et al. (2018). Shared and distinct transcriptomic cell types across neocortical areas. *Nature* 563, 72–78. doi: 10.1038/s41586-018-0654-5
- Teles-Grilo Ruivo, L. M., Baker, K. L., Conway, M. W., Kinsley, P. J., Gilmour, G., Phillips, K. G., et al. (2017). Coordinated Acetylcholine Release in Prefrontal Cortex and Hippocampus Is Associated with Arousal and Reward on Distinct Timescales. *Cell Rep.* 18, 905–917. doi: 10.1016/j.celrep.2016.12.085
- Tian, M. K., Bailey, C. D., and Lambe, E. K. (2014). Cholinergic excitation in mouse primary vs. associative cortex: region-specific magnitude and receptor balance. *Eur. J. Neurosci.* 40, 2608–2618. doi: 10.1111/ejn.12622
- Turrini, P., Casu, M. A., Wong, T. P., De Koninck, Y., Ribeiro-da-Silva, A., and Cuello, A. C. (2001). Cholinergic nerve terminals establish classical synapses in the rat cerebral cortex: synaptic pattern and age-related atrophy. *Neuroscience* 105, 277–285. doi: 10.1016/s0306-4522(01)00172-5
- Unwin, N. (2003). Structure and action of the nicotinic acetylcholine receptor explored by electron microscopy. *FEBS Lett.* 555, 91–95. doi: 10.1016/s0014-5793(03)01084-6
- Veit, J., Hakim, R., Jadi, M. P., Sejnowski, T. J., and Adesnik, H. (2017). Cortical gamma band synchronization through somatostatin interneurons. *Nat. Neurosci.* 20, 951–959. doi: 10.1038/nn.4562
- Wang, X., Tucciarone, J., Jiang, S., Yin, F., Wang, B. S., Wang, D., et al. (2019). Genetic Single Neuron Anatomy Reveals Fine Granularity of Cortical Axo-Axonic Cells. *Cell Rep.* 26, 3145–59e5. doi: 10.1016/j.celrep.2019.02.040
- Xiang, Z., Huguenard, J. R., and Prince, D. A. (1998). Cholinergic switching within neocortical inhibitory networks. *Science* 281, 985–988. doi: 10.1126/science.281.5379.985
- Xu, H., Jeong, H. Y., Tremblay, R., and Rudy, B. (2013). Neocortical somatostatin-expressing GABAergic interneurons disinhibit the thalamorecipient layer 4. *Neuron* 77, 155–167. doi: 10.1016/j.neuron.2012.11.004
- Yang, D., Günter, R., Qi, G., Radnikow, G., and Feldmeyer, D. (2020). Muscarinic and Nicotinic Modulation of Neocortical Layer 6A Synaptic Microcircuits Is Cooperative and Cell-Specific. *Cereb. Cortex* 30, 3528–3542. doi: 10.1093/cercor/bhz324
- Yuste, R., Hawrylycz, M., Aalling, N., Aguilar-Valles, A., Arendt, D., Armananzas, R., et al. (2020). A community-based transcriptomics classification and nomenclature of neocortical cell types. *Nat. Neurosci.* 23, 1456–1468. doi: 10.1038/s41593-020-0685-8
- Zaborszky, L., Csordas, A., Mosca, K., Kim, J., Gielow, M. R., Vadasz, C., et al. (2015). Neurons in the basal forebrain project to the cortex in a complex topographic organization that reflects corticocortical connectivity patterns: an experimental study based on retrograde tracing and 3D reconstruction. *Cereb. Cortex* 25, 118–137. doi: 10.1093/cercor/bht210
- Zeng, H., and Sanes, J. R. (2017). Neuronal cell-type classification: challenges, opportunities and the path forward. *Nat. Rev. Neurosci.* 18, 530–546. doi: 10.1038/nrn.2017.85
- Zolles, G., Wagner, E., Lampert, A., and Sutor, B. (2009). Functional expression of nicotinic acetylcholine receptors in rat neocortical layer 5 pyramidal cells. *Cereb. Cortex* 19, 1079–1091. doi: 10.1093/cercor/bhn158

Conflict of Interest: The authors declare that the research was conducted in the absence of any commercial or financial relationships that could be construed as a potential conflict of interest.

Publisher's Note: All claims expressed in this article are solely those of the authors and do not necessarily represent those of their affiliated organizations, or those of the publisher, the editors and the reviewers. Any product that may be evaluated in this article, or claim that may be made by its manufacturer, is not guaranteed or endorsed by the publisher.

Copyright © 2022 Qi and Feldmeyer. This is an open-access article distributed under the terms of the Creative Commons Attribution License (CC BY). The use, distribution or reproduction in other forums is permitted, provided the original author(s) and the copyright owner(s) are credited and that the original publication in this journal is cited, in accordance with accepted academic practice. No use, distribution or reproduction is permitted which does not comply with these terms.